INVESTIGATION OF SOME GALACTIC AND EXTRAGALACTIC GRAVITATIONAL PHENOMENA

P. Jovanović

Astronomical Observatory, Volgina 7, 11060 Belgrade 38, Serbia
E–mail: *pjovanovic@aob.rs*

SUMMARY: Here we present a short overview of the most important results of our investigations of the following galactic and extragalactic gravitational phenomena: supermassive black holes in centers of galaxies and quasars, supermassive black hole binaries, gravitational lenses and dark matter. For the purpose of these investigations, we developed a model of a relativistic accretion disk around a supermassive black hole, based on the ray-tracing method in the Kerr metric, a model of a bright spot in an accretion disk and three different models of gravitational microlenses. All these models enabled us to study physics, spacetime geometry and effects of strong gravity in the vicinity of supermassive black holes, variability of some active galaxies and quasars, different effects in the lensed quasars with multiple images, as well as the dark matter fraction in the Universe. We also found an observational evidence for the first spectroscopically resolved sub-parsec orbit of a supermassive black hole binary system in the core of active galaxy NGC 4151. Besides, we studied applications of one potential alternative to dark matter in the form of a modified theory of gravity on Galactic scales, to explain the recently observed orbital precession of some S-stars, which are orbiting around a massive black hole at the Galactic center.

Key words. gravitation – gravitational lensing: micro – dark matter – black hole physics – galaxies: active – accretion, accretion disks – galaxy: center – stars: individual: S2.

1. INTRODUCTION

On the largest scale, the Universe can be considered as a homogeneous and isotropic medium in the state of accelerated expansion, but on the scales up to 100 Mpc it looks inhomogeneous with hierarchical structure in which stars are organized into galaxies, galaxies are grouped into clusters, which in turn form superclusters and filaments of galaxies, separated by immense voids. Gravitation, the weakest of the four forces of nature, plays a substantial role in formation of such hierarchical large scale structure of the Universe, and therefore, it is of essential significance in modern astrophysics and cos-mology to study different gravitational phenomena at galactic, extragalactic and cosmological scales.

Some of the most intriguing such gravitational phenomena are supermassive black holes in centers of galaxies and quasars, supermassive black hole binaries originating in galactic mergers, gravitational lenses, dark matter and its potential alternatives. To investigate them, we performed different theoretical studies, numerical modeling/simulations and comparisons of the obtained simulated results with observations by ground-based and space-based astronomical detectors, as well as with data from different astronomical databases. In the following we present some of the most important results of these investigations.
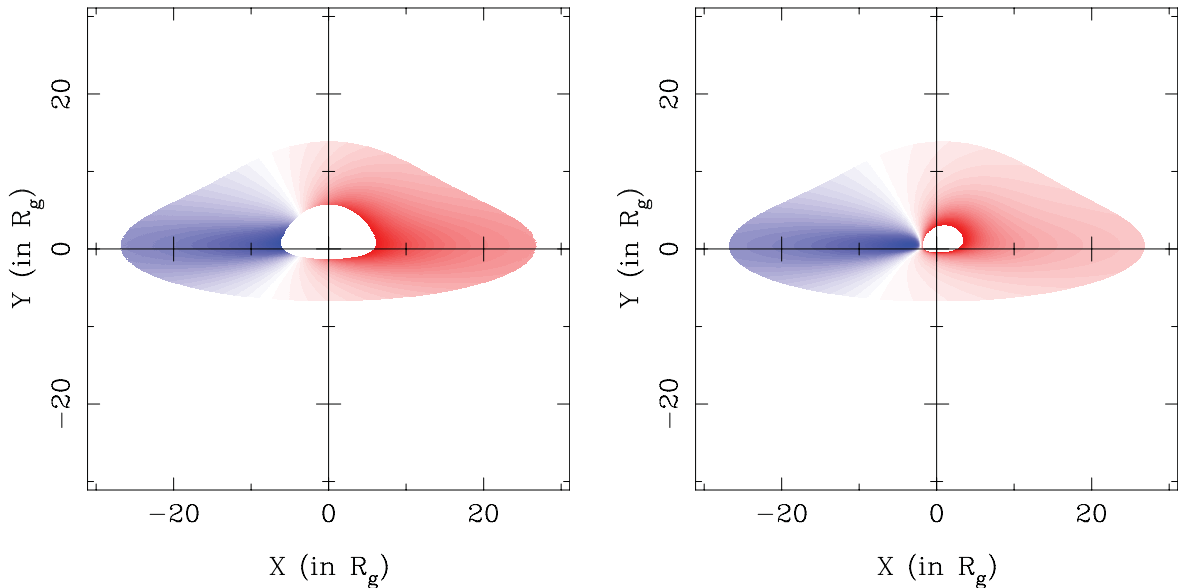
Fig. 1. *Simulated images of two highly inclined (i = 75°) accretion disks around a Schwarzschild (left) and an extreme (i.e. maximally rotating) Kerr SMBH (right). Both disks extend from the marginally stable orbit around the SMBH up to 30 R_g, where the gravitational radius R_g is equal to one half of the Schwarzschild radius.*

2. SUPERMASSIVE BLACK HOLES

According to the general relativity, a black hole is a region of spacetime around a collapsed mass with a gravitational field that has became so strong that nothing (including the electromagnetic radiation) can escape from its attraction, after crossing its event horizon (Wald 1984). Black holes have only three measurable parameters, not including the Hawking temperature (Yaqoob 2007): the charge, mass and angular momentum (spin). Therefore, they can be classified according to the metrics which describes the spacetime geometry around them (i.e. according to the corresponding solutions of the field equations of the general relativity) into the following four types:

(i) Schwarzschild (non-rotating and uncharged).
(ii) Kerr (rotating and uncharged).
(iii) Reissner-Nordström (non-rotating and charged).
(iv) Kerr-Newman (rotating and charged).

Besides, all the black holes in nature are commonly classified according to their masses as (see e.g. Jovanović 2012a):

(i) Mini, micro or quantum mechanical: $M_{BH} \ll M_\odot$ (primordial black holes in the early Universe).
(ii) Stellar-mass: $M_{BH} < 10^2 \, M_\odot$ (located in the X-ray binary systems).
(iii) Intermediate-mass: $M_{BH} \sim 10^2 - 10^5 \, M_\odot$ (located in the centers of globular clusters).
(iv) Supermassive: $M_{BH} \sim 10^5 - 10^{10} \, M_\odot$ (located in the centers of all galaxies, including ours).

It is now widely accepted that most galaxies harbor a supermassive black hole (SMBH) in their centers and that the formation and evolution of galaxies is fundamentally influenced by properties of their central SMBHs. For example, active galaxies, which most likely represent one phase in evolution of any galaxy, derive their extraordinary luminosities from energy release by matter accreting towards, and falling into, a central SMBH through an accretion disk, which represents an efficient mechanism for extracting gravitational potential energy and converting it into radiation. In the case of such SMBHs, only their masses and spins are of sufficient importance because they are responsible for several effects, which can be observationally detected (see e.g. Jovanović and Popović 2008a). Therefore, the spacetime geometry around SMBHs is usually described by the Schwarzschild or Kerr metrics.

2.1. Relativistic accretion disks around supermassive black holes

Our studies of SMBHs were mostly concentrated to accretion processes and effects of strong gravity in their vicinity (see e.g. Jovanović and Popović 2008a, Jovanović et al. 2010). For that purpose, we developed a code to perform numerical simulations of radiation from relativistic accretion disks around SMBHs, based on the ray-tracing method in Kerr metric. By this code we were able to obtain colorful simulated images of such accretion disks as would be seen by a distant observer with a powerful high-resolution telescope (see Fig. 1). As one can see from Fig. 1, the radius of the innermost circular orbit (the so called marginally stable orbit) strongly depends on the SMBH spin, and consequently, affects the radiation originating from the innermost regions of the disk.
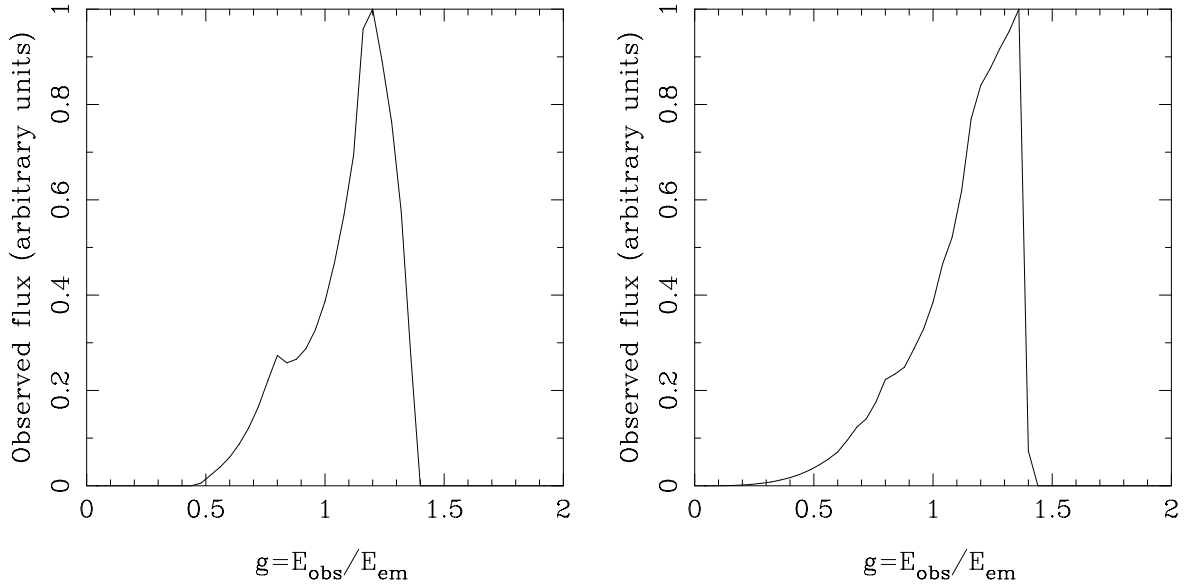
Fig. 2. *Simulated profiles of the Fe Kα spectral line emitted from two accretion disks presented in Fig. 1.*

2.2. The broad Fe Kα spectral line

The innermost regions of a relativistic accretion disk radiate in the X-ray spectral band and the most prominent X-ray feature is a broad emission, double peaked Fe Kα spectral line at 6.4 keV, which has an asymmetric shape with narrow bright blue and wide faint red peak. Since this line is produced close to the marginally stable orbit, it is an important indicator of accreting flows around SMBHs, as well as of the spacetime geometry in these regions (for more details, see Jovanović 2012a). In the case of some active galaxies, its Full-Width at the Half-Maximum (FWHM) corresponds to relativistic velocities, which sometimes reach 30% of the speed of light. Therefore, its complex profile is a result of combination of three different effects (Jovanović 2012a):

(i) Doppler shift due to rotation of emitting material, which is responsible for occurrence of two peaks;

(ii) Special relativistic effect, known as the relativistic beaming, which is responsible for enhancement of the blue peak with respect to the red one;

(iii) General relativistic effect, known as the gravitational redshift, which is responsible for smearing of the line profile.

Fig. 2. presents two simulated profiles of the Fe Kα spectral line originating from two accretion disks presented in Fig. 1. As it can be seen from Fig. 2, the two different spacetime geometries (metrics) significantly affect the line shape.

Comparisons between such simulations and the corresponding observations enabled us to obtain some properties of the SMBHs (e.g. their masses and spins), located at centers of certain galaxies and quasars. Also, the parameters of accretion disks around these SMBHs (such as their size, inclination,

emissivity, accretion rate, etc) were also studied in order to reveal the physics and structure of central parts of galaxies and quasars, as well as to get information about their activity, evolution and observational signatures (Jovanović 2012a).
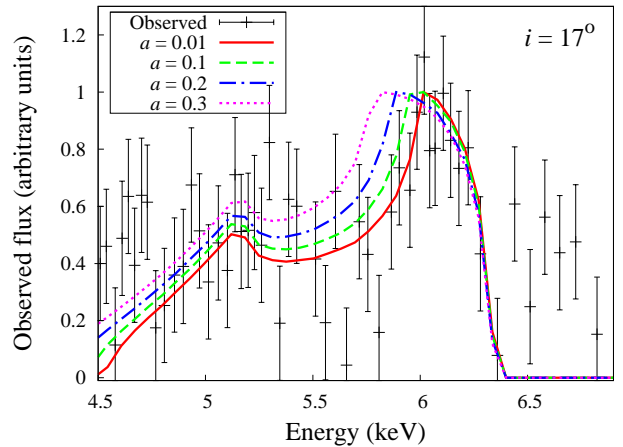

Fig. 3. *Comparison between the observed and simulated profiles of the Fe Kα line in the case of 3C 405 (Jovanović et al. 2011). Chandra observations (Wilson et al. 2001) are denoted with black crosses with error bars, while the corresponding simulated profiles for 4 different values of the black hole spin are denoted with color lines.*

For example, in order to contribute to our understanding of possible causes of systematic difference in the Fe Kα line emission between radio-quiet and radio-loud active galaxies (see e.g. Gambill et al. 2003), we investigated properties of their central SMBHs. Namely, the Fe Kα line emission is a well known property of radio-quiet active galaxies,

but it is very rare in the case of radio-loud class of these objects. For that purpose we studied the Fe Kα line in the case of a radio-loud active galaxy 3C 405 (Cygnus A), since it represents an exception from this rule, mostly due to its proximity ($z = 0.0562$). Therefore, we estimated the spin of the central black hole of 3C 405 by comparing its simulated Fe Kα line profiles with the corresponding profiles observed by Chandra (Wilson et al. 2001).

The obtained results are presented in Fig. 3 (see Jovanović et al. 2011. for more details). As it can be seen from Fig. 3, the best fit was obtained for a very slowly rotating or even a stationary black hole and for a slightly inclined accretion disk ($i = 17°$), extending from the radius of the marginally stable orbit up to 10 R_g.

2.3. Variability due to perturbations in the emissivity of relativistic accretion disks

We also studied the radiation emitted from the accretion disks in different spectral bands, its properties and causes of its variability (see e.g. Jovanović and Popović 2009a, Bon et al. 2009, and references therein), as the observed variability can give us information on violent physical processes, which occur in centers of active galaxies and quasars.

The variability of spectral lines emitted from accretion disk could be caused by instability in the disk itself. Therefore, assuming that this instability in the disk affects its emissivity, we developed a model of emissivity perturbation in the form of a single bright spot (or flare) by a modification of the power law disk emissivity (Jovanović and Popović 2008b, Stalevski et al. 2008, Jovanović and Popović 2009b, Jovanović et al. 2010). A 3D plot of the modified emissivity law is given in Fig. 4 (Jovanović et al. 2010).
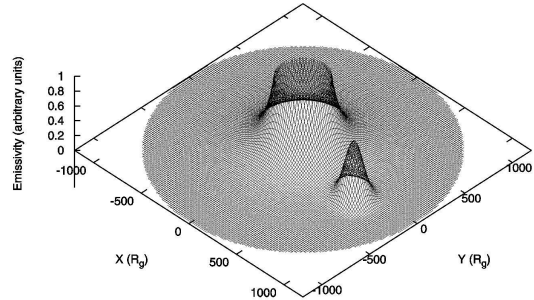

Fig. 4. *Modified power law emissivity in the case of a bright spot in accretion disk which extends from 200 up to 1200 R_g (Jovanović et al. 2010).*

This simple model allowed us to change amplitude, width and location of bright spot with respect to the disk center. In that way, we were able to simulate the displacement of a bright spot along the disk, its widening and amplitude decrease with time (decay).

We then used this model to simulate the variability of double peaked line profiles, emitted from accretion disk of active galaxies and quasars (Jovanović et al. 2010). In order to test how this model of a bright spot affects the line profiles, we performed several numerical simulations of perturbed emission of an accretion disk in Kerr metric for different positions of the bright spot along the x and y-axes in both, positive and negative directions, as well as along the $y = x$ direction (see Fig. 5).
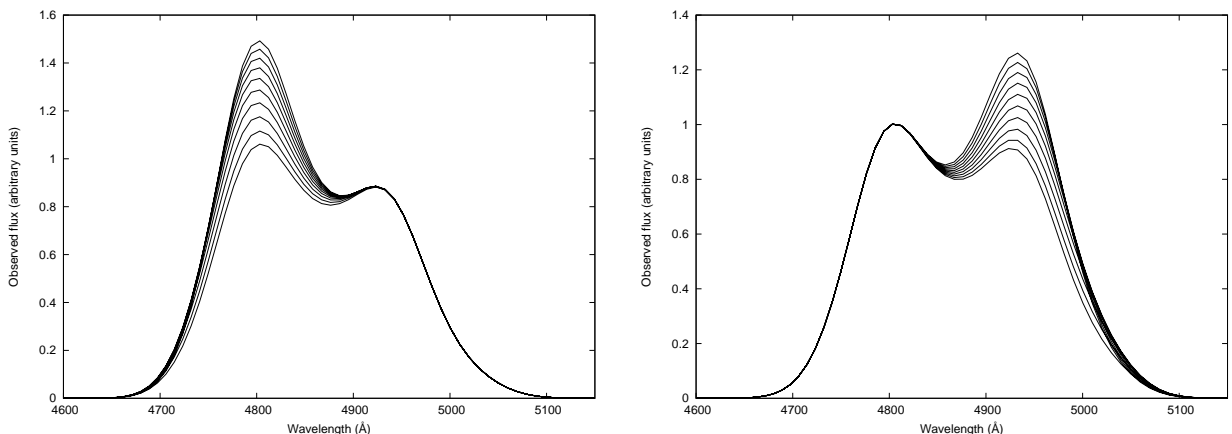

Fig. 5. *Variations of the perturbed Hβ line profile for different positions of the bright spot along the $y = x$ direction (Jovanović et al. 2010). Left panel corresponds to positions of the bright spot on the approaching side of the disk, while the right panel corresponds to the receding side of the disk. In both cases, the positions of the bright spot were varied from the inner radius of the disk (bottom profiles) towards its outer radius (top profiles).*

This model can successfully explain some differences in double peaked line profiles, such as e.g. a higher red peak even in the case of the standard circular disk (see Fig. 5). The position of a bright spot has a stronger influence on one particular part of the spectral line profile (e.g. on its core if the spot is in the central part of the disk, or on "red" and "blue" wings if the spot is located on the receding and approaching part, respectively).

This model has been used to successfully model and reproduce the observed variations of the Hβ line profile in the case of quasar 3C 390.3, including the two large amplitude outbursts, which occurred during the observed period (Jovanović et al. 2010). We showed that these two outbursts could be explained by successive occurrences of two different bright spots on the approaching side of the disk, which originate in the inner regions of the disk and spiral outwards, decaying by time until they completely disappear.

2.4. Photocentric variability of quasars

We also used this bright spot model to study variations of quasar photocenters, caused by an outburst in their accretion disks, in the context of the future Gaia mission (Popović et al. 2012). The Gaia mission aims to determine high-precision astrometric parameters for one billion objects with apparent magnitudes in the range $5.6 \leq V \leq 20$ (see e.g. Perryman et al. 2001, Lindegren et al. 2008). Among these objects about 500 000 quasars are going to be observed. Some of these quasars will be used for construction of a dense optical QSO-based celestial reference frame (see Bourda et al. 2010) and, therefore, their intrinsic photocenter position stability must be investigated at the sub-mas level. However, they are active galactic nuclei powered by SMBHs and, hence, some effects in their accretion disks could affect precise determination of their photocenters. This motivated us to investigate astrometric stability of the quasars.

Table 1. The simulated offsets of the photocenter (in mas), caused by a perturbation in accretion disk, for different values of redshift and mass of a central black hole (Popović et al. 2012).

M_{BH}	z				
($M_{\odot}$)	0.01	0.05	0.10	0.15	0.20
10^8	0.036	0.007	0.004	0.003	0.002
10^9	0.355	0.074	0.039	0.028	0.022
10^{10}	3.550	0.744	0.394	0.278	0.220

We considered a perturbation (or the bright spot) at a certain part of the disk, for different values of the spot brightness, and calculated the photocenter of the accretion disk as a centroid of the observed flux over the disk image. The results for different redshifts and masses of a central SMBH are given numerically in Table 1, and those for different emissivities of the accretion disk located at $z = 0.01$

around a SMBH with mass of 10^{10} $M_{\odot}$ are graphically presented in Fig. 6 (Popović et al. 2012). The maximum emissivity of the perturbing region is taken to be ten times greater than that of the emissivity of the disk at its inner radius.
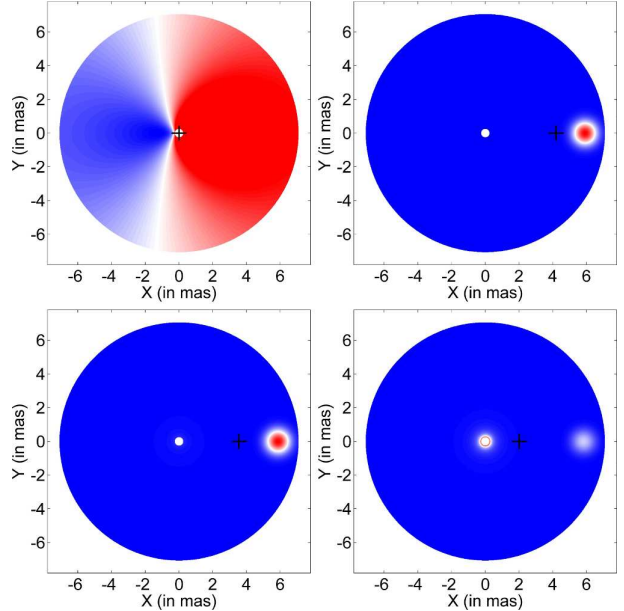

Fig. 6. *Simulations of an accretion disk without (top left) and with the perturbation for three different values of emissivity index: 0 (top right), -1 (bottom left), and -2 (bottom right). The photocenter positions are denoted by crosses. In the top left panel, color represents the energy shift due to relativistic effects (i.e. ratio between the observed and emitted energy), while in the other three panels it represents the observed flux in arbitrary units (Popović et al. 2012).*

These results show that bright spots in accretion disk could cause a maximal offset of the quasar photocenter of a few mas in the case when such a bright spot is located at the disk edge. Thus, this effect has a good chance to be detected by the Gaia mission (Popović et al. 2012). The most likely candidates are low-redshifted quasars with massive central SMBHs ($10^9 - 10^{10}$ $M_{\odot}$), which are, in principle, very bright objects.

3. SUPERMASSIVE BLACK HOLE BINARIES

Supermassive black hole binaries (SMBHBs) originate in galactic mergers and their coalescences represent the most powerful sources of gravitational waves. There are the three main phases of a SMBHB coalescence (see e.g. Bogdanović et al. 2008):

(i) The first phase in evolution of a SMBHB is the galactic merger, during which two SMBHs, initially carried within their host bulges, even-
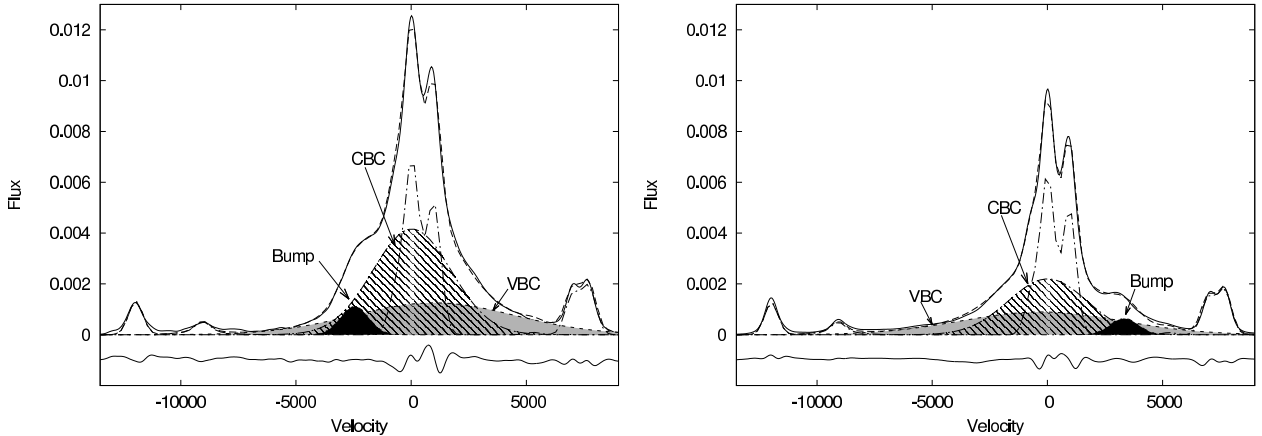
Fig. 7. *Two examples of the best fits (dashed line) with a sum of three Gaussian components (denoted as VBC, CBC and bump) of the Hα line profile (solid line) for two epochs: MJD 51203 (left) and MJD 52621 (right) (Bon et al. 2012).*

tually find themselves at ∼kpc separation from each other and spiral together on quasicircular orbits.

(ii) During the second stage, the two SMBHs become gravitationally bound, falling towards the center and merge together, forming a common horizon.

(iii) The third and final stage is when nonaxisymmetric modes of this distorted remnant are removed by the emission of gravitational waves, forming a single Kerr SMBH with mass slightly lower (typically by several percent) than that of the two parent SMBHs combined.

It is believed that gravitational waves carry a tremendous amount of information through the Universe, and they are expected to be detected in near future by ground-based or space-based interferometers. Therefore, they are the main research subject of the emerging field of gravitational wave astronomy. Electromagnetic counterparts of gravitational waves emitted during coalescences of SMBHBs represent the most direct evidence of their formation, as well as their essential observational signatures (see e.g. Bogdanović et al. 2009).

In our previous investigations, we studied observational signatures of SMBHBs, and one of the most important results in this field was a recently found observational evidence of the first spectroscopically resolved sub-parsec orbit of a such system in the core of active galaxy NGC 4151 (Bon et al. 2012). We used a method similar to those typically applied to the spectroscopic binary stars to obtain radial velocity curves of the SMBHB, from which we then calculated orbital elements and estimated masses of the components. We analyzed the variability of the Hα spectral line of NGC 4151 during the period of more than 20 years and interpreted the detected periodicity in terms of orbital motion of central SMBH at sub-parsec scales.

The line profile variations were first studied by decomposing each observed Hα profile into the following three Gaussian components (see Fig. 7): a very broad component (VBC) corresponding to the far wings, a central broad component (CBC) corresponding to the broad line core and an intermediate width component (bump) appearing either on the blue or red wing of each Hα line profile (Bon et al. 2012). Such composite line profiles are expected in the case of SMBHBs according to some previous theoretical studies (see e.g. Popović 2012).

We then analyzed radial velocities of the VBC and bump components, and found that the obtained radial velocity curves are consistent with an eccentric Keplerian orbit of a binary system (see Fig. 8).
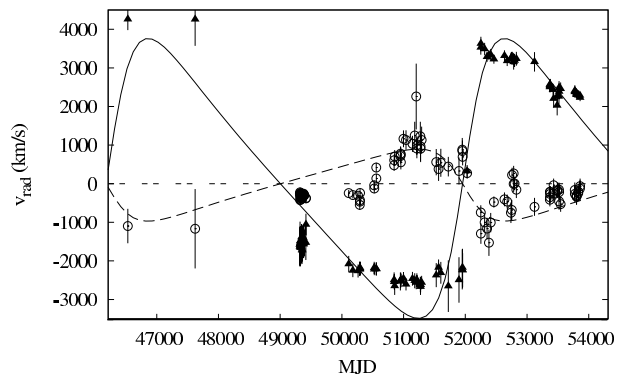

Fig. 8. *Radial velocities of the bump (triangles) and VBC (circles) obtained from Gaussian decomposition of the broad Hα line, as well as fitted radial velocity curves for both components (solid and dashed lines) (Bon et al. 2012).*

Therefore, we used these radial velocity curves to obtain the following Keplerian orbital elements (Bon et al. 2012): the orbital period $P = 5776$ days, eccentricity $e = 0.42$, longitude of pericenter $\omega \approx 95°$, the semimajor axes: $a_1 \sin i = 0.002$ pc, $a_2 \sin i = 0.008$ pc and masses of the components:

$m_1 \sin^3 i = 3 \times 10^7 M_\odot$ and $m_2 \sin^3 i = 8.5 \times 10^6 M_\odot$. Some previous studies indicated that the inclination i of the orbital plane could be about $65°$, which resulted into the following semimajor axes: 0.0024 pc and 0.0094 pc (i.e. with the separation between components of about 0.01 pc), and masses of the components: $4.4 \times 10^7 M_\odot$ and $1.2 \times 10^7 M_\odot$. These mass estimates were in good agreement with those previously obtained from reverberation mapping (see e.g. Onken et al. 2007).

These results suggested that many such SMBHBs may exist in similar active galaxies, whose binarity could be a necessary condition for triggering their activity.

4. GRAVITATIONAL LENSING

Gravitational lensing is another natural phenomenon where the gravitational force of a massive foreground object deflects the light rays from distant background sources. Depending on the mass of lensing objects, they can produce multiple images of background sources (in the case of lensing by galaxies), their images in form of giant arcs (in the case of lensing by clusters of galaxies) or just their amplification (in the case of lensing by compact objects, such as normal stars, brown dwarfs or even planets). In the last case, which is called microlensing, the separation between the images of a background source is of the order of several μas, and therefore not resolvable by present telescopes. All these effects are commonly called - a strong lensing.

However, in some cases, the deflection of light caused by the foreground matter is not sufficiently large to produce neither multiple images, nor significant amplification of distant background sources. Instead, the trajectories of photons emitted by them are perturbed by the inhomogeneous distribution of the foreground matter, and therefore, the shapes of these sources appear to us slightly distorted in comparison with the corresponding shapes, which would appear in a perfectly homogeneous and isotropic Universe. Such phenomenon is called a weak gravitational lensing. A similar effect caused by substructures in a lensing galaxy is referred to as a gravitational millilensing.

Both the strong and weak gravitational lensing have a wide range of applications which include:
  (i) detection of distant objects (Richard et al. 2011),
 (ii) constraining cosmological parameters (Oguri et al. 2012, Cao et al. 2012, Jovanović and Popović, 2010 and references therein),
(iii) studies of the dark and visible matter distribution (Massey et al. 2007, Zakharov et al. 2004),
 (iv) investigation of innermost regions of active galaxies (see e.g. Jovanović et al. 2009), and
  (v) detection of extrasolar planets, not only in our Galaxy, but even in nearby galaxies such as

Andromeda and Magellanic Clouds (see e.g. Ingrosso et al., 2009, Zakharov, 2009).

The gravitational lensing is related to a number of still unsolved problems. For example, cosmological studies based on gravitational lensing statistics and time delays usually underestimate values of Ω_Λ and H_0, indicating a lower content of dark energy and older Universe, respectively (see e.g. Jackson 2007). Also, recent studies of gravitational lensing by clusters of galaxies resulted in discoveries of galaxies at redshifts higher than 10 (see e.g. Stark et al. 2007), only few Myr after the Big Bang and close to the "dark ages", according to the standard ΛCDM cosmological model. Potential discoveries of even more distant galaxies would result in a lack of time for galaxy formation and reopen a question about the age of the Universe.

In our previous investigations, we performed both observations of gravitational lenses (see e.g. Popović et al. 2010), as well as theoretical studies of their different aspects. Our theoretical investigations were mostly focused on gravitational microlenses and their influence on radiation from relativistic accretion disks around the central SMBHs of distant quasars, their cosmological distribution and statistics, as well as their influence on radiation in different spectral bands emitted from lensed quasars with multiple images.

For that purpose we developed three models of gravitational microlenses:
  (i) a point-like microlens – for studying microlensing by an isolated compact object (see e.g. Popović et al. 2001, Jovanović et al. 2003),
 (ii) a straight-fold caustic – for studying microlensing by a number of microdeflectors located within an extended object (see Jovanović et al. 2008 and references therein), and
(iii) a microlensing map (pattern) or caustic network – the most realistic model, which is usually applied in obtaining a spatial distribution of magnifications in the source plane (where a quasar is located), produced by randomly distributed stars in the lensing galaxy (Jovanović et al. 2008 and references therein).

4.1. Influence of gravitational microlenses on radiation from relativistic accretion disks around SMBHs

An illustration of a point-like gravitational microlens crossing over an accretion disk in the Kerr metric with angular momentum $a = 0.998$ is presented in top left panel of Fig. 9, and the corresponding illustration of a straight-fold caustic crossing over a disk in Schwarzschild metric in the top right panel of the same figure. The influence of the straight-fold caustic on the shapes of the X-ray continuum and the Fe Kα line are shown in the bottom panel of Fig. 9 (Jovanović 2006).
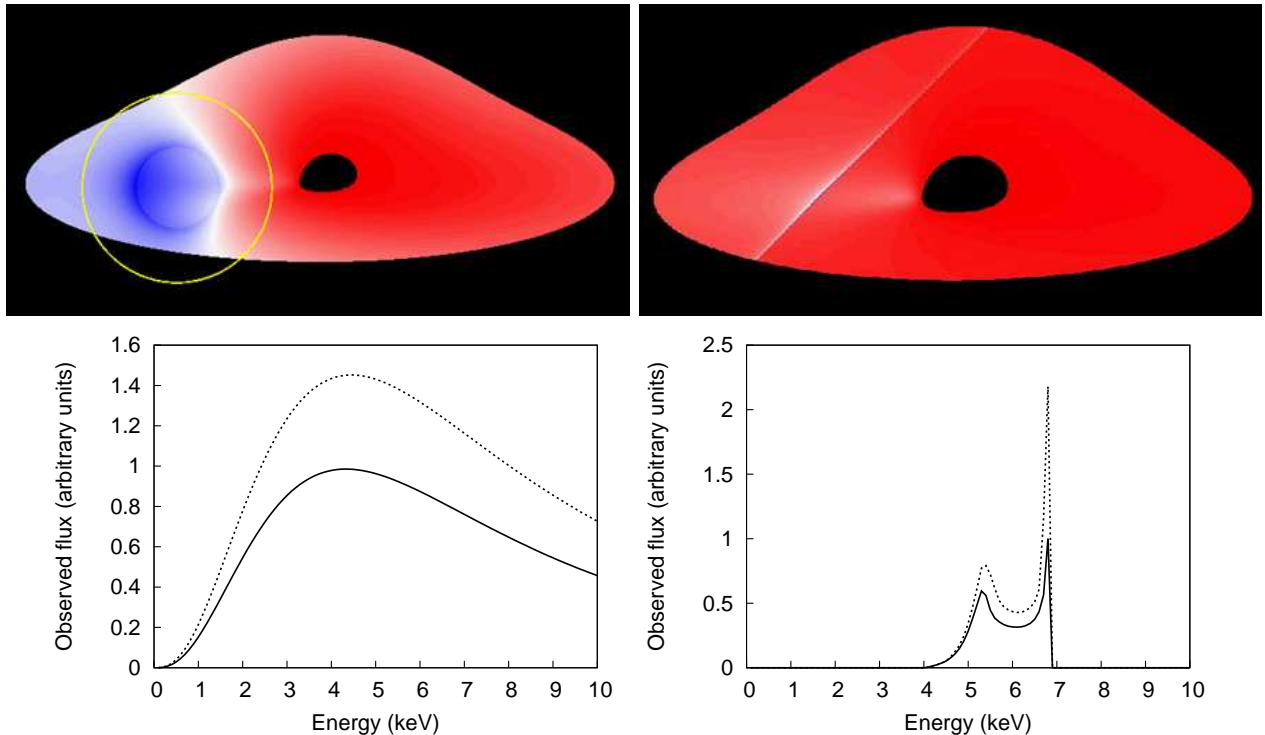
Fig. 9. *Top: illustrations of a point-like (left) and a straight-fold caustic (right) gravitational microlens crossing over a relativistic accretion disk in extreme Kerr and Schwarzschild metric, respectively. Bottom: comparisons between the undeformed (solid lines) and deformed (dashed lines) shapes of the X-ray continuum (left) and the Fe Kα spectral line (right) due to the influence of the straight-fold caustic presented in the top right panel (Popović et al. 2003a, Jovanović 2006).*

As it can be seen from Fig. 9, depending on the location of the microlenses, they could induce significant changes of the shape and amplifications of the intensity of both the X-ray continuum and Fe Kα spectral line. Also, due to a small size of the X-ray emitting region, even very compact objects with small masses could induce a significant variability of the X-ray radiation emitted from relativistic accretion disks around SMBHs.

4.2. Gravitational microlenses in multiple imaged quasars

Gravitationally lensed quasars represent a particularly interesting systems since the different lensing regimes can be present in them: a strong lensing by a lens galaxy, microlensing by stars in a lens galaxy (see e.g. Jovanović 2005), and millilensing due to the cold dark matter (CDM) substructures in a lens galaxy. Also, in a number of lensed systems, the flux ratios between their images deviate from those predicted by simple lens models (see e.g. Goldberg et al. 2010). One of the possible causes for this, so called the flux anomaly, is a microlensing by stars in the lens galaxy (see e.g. Simić et al. 2011). Therefore, the lensed quasars with multiple images represent a powerful tool for studying the structure of both the lens galaxy and the background quasar.

For some specific lensing event one can model the corresponding magnification map by using numerical simulations based on the ray-shooting technique (see e.g. Jovanović et al. 2008 and references therein), in which the rays are shot from the observer to the source, through a randomly generated star field in the lens plane. An example of such magnification map for a "typical" lens system (i.e. for a system where the redshifts of the lens and source are $z_l = 0.5$ and $z_s = 2$, respectively) is presented in the left panel of Fig. 10, and the corresponding X-ray, UV and optical continuum variations are given in the right panel of the same figure (Jovanović et al. 2008). The simulated light curves in the right panel of Fig. 10 are produced for an accretion disk crossing over the magnification pattern in the left panel, along the path denoted by the white solid line.

As one can see from the right panel of Fig. 10, the variations of the X-ray continuum due to microlensing are much stronger and faster in comparison to the variations in UV and optical spectral bands. The so called high amplification events, i.e. the asymmetric peaks in the light curves, were also analyzed, and it was shown that the rise times of such events are the shortest and their frequency the highest in the X-rays, in comparison to the UV/optical spectral bands. The typical microlensing time-scales for the X-ray band are on the order of several months while those for the UV/optical band are of the order of several years (Jovanović et al. 2008).
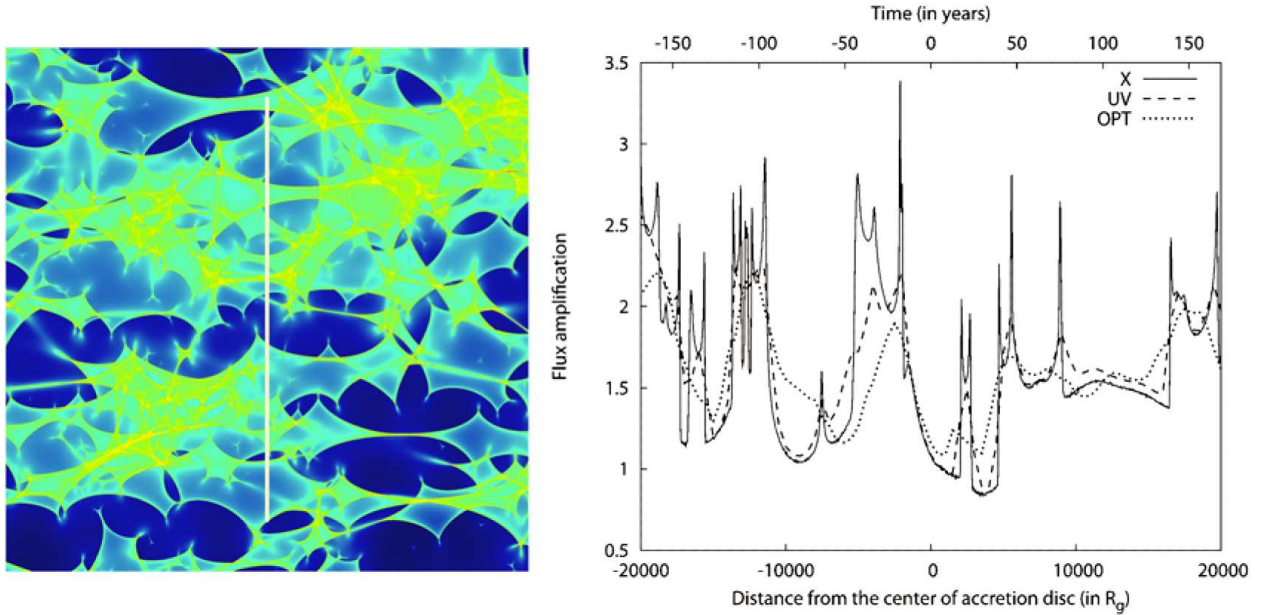
Fig. 10. *Left: Magnification map of a "typical" lens system, where the white solid line represents a path of an accretion disk center. Right: Variations in the X-ray (solid), UV (dashed) and optical (dotted) spectral bands caused by the crossing of the accretion disk along the specified path (Jovanović et al. 2008).*

These investigations also showed that the size of the source has a large effect on variations due to microlensing. As an extended source covers a larger area of a microlensing magnification pattern at any given time than a point source, its brightness varies less as it moves relative to the lens and observer (Mortonson et al. 2005). A lensed source is significantly affected by microlensing only if the source is smaller than the relevant microlensing length scale (the Einstein ring radius). Since the sizes of different emitting regions of quasars are wavelength-dependent, microlensing by stars in the lens galaxy will lead to a wavelength-dependent magnification. The X-ray radiation is coming from a very compact region in the innermost part of the accretion disk, and therefore, it will be magnified more and its variations will be faster than for the radiation in the UV and optical bands, coming from outer, larger parts of the disk (Jovanović et al. 2008). Thus, although the gravitational lensing is an achromatic phenomenon, due to the complex structure of emission regions, "the chromatic" effect may arise in the lensed quasar systems (Popović et al. 2006, Jovanović et al. 2008).

We also investigated the influence of gravitational microlensing on infrared radiation from the lensed quasars (see Stalevski et al. 2012). Infrared spectra of most quasars are dominated by thermal emission from hot dust in their tori, or alternatively, by nonthermal synchrotron emission from regions near their central black holes. The variability in the infrared band due to gravitational microlensing could be used to constrain the size of the infrared emission region, and hence to distinguish between the thermal and synchrotron mechanisms. If the infrared radiation varies on timescales shorter than decades, then its emission region is smaller, located closer to the central black hole, and its emission is nonthermal, while longer timescales indicate a larger, thermal region (see Stalevski et al. 2012 and references therein). Additionally, chromatic effects in the infrared band have been observed in some of the lensed quasars, where the color differences between their multiple images were detected, and the most realistic scenario that can explain the observed color differences is gravitational microlensing.

To study these effects, we modeled the dusty torus as a clumpy two-phase medium (see Stalevski et al. 2012. for more details). We used the 3D Monte Carlo radiative transfer code SKIRT (Baes et al. 2003) to obtain spectral energy distributions and images of tori at different wavelengths. The obtained images of the torus at different wavelengths are presented in the top row of Fig. 11 (Stalevski et al. 2012). Microlensing by stars in the lens galaxy was simulated using the magnification map, which was calculated for a point source by the ray-shooting technique. As the dusty tori were larger than the typical size of microlens, they were treated as extended sources, and to take this into account, the magnification map was convolved with the images of the torus at different wavelengths. The bottom row of Fig. 11 shows the magnification maps after convolution with the corresponding torus images from the top row.
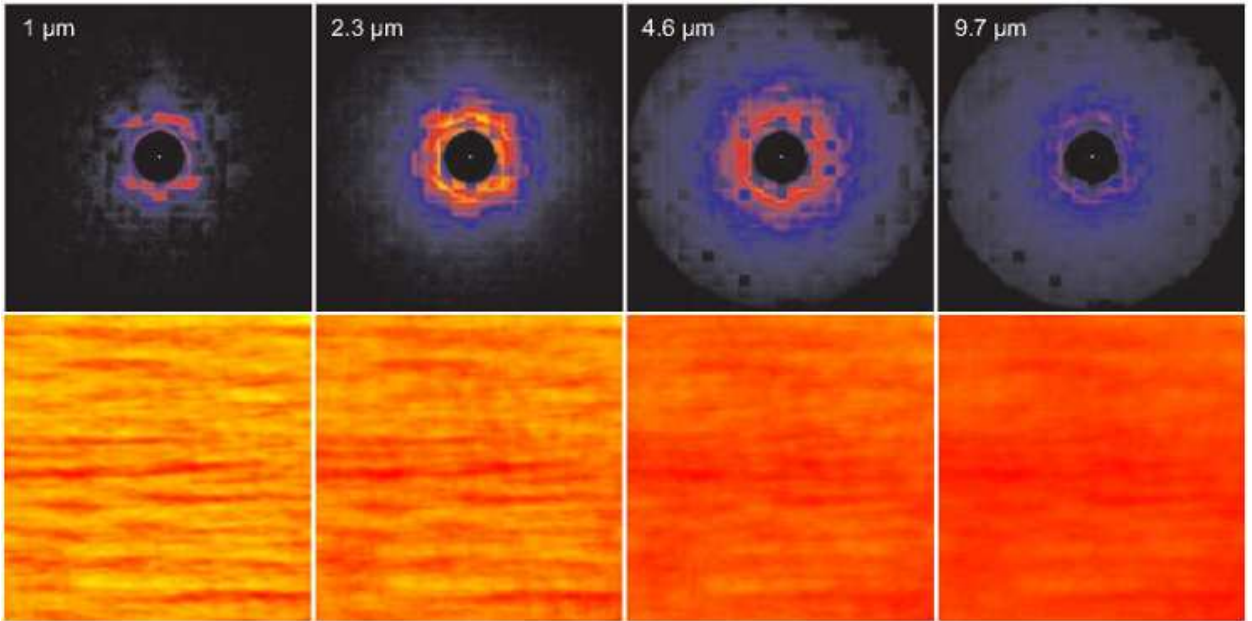
Fig. 11. *Simulated images of a torus with the face-on orientation at four different wavelengths in the infrared band (top), and the microlensing magnification maps (bottom) after convolution with the corresponding tori images from the top row (Stalevski et al. 2012).*

The obtained simulated microlensing light curves for a source at redshift of $z_s = 2$ and the lens galaxy at redshift $z_l = 0.05$ are presented in Fig. 12 (Stalevski et al. 2012). It can be seen from Fig. 12 that dusty tori could be significantly magnified by gravitational microlensing. As a consequence of the wavelength dependency of the torus size, the magnification amplitude of the microlensing events is also wavelength dependent. The magnification was highest at near-infrared wavelengths and decreased toward the far-infrared range.
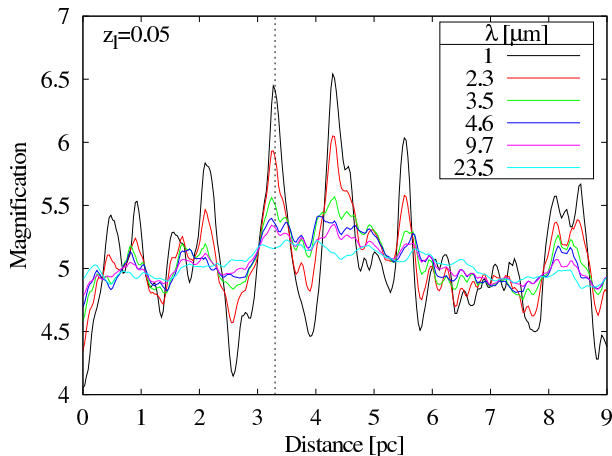

Fig. 12. *Simulated light curves for magnification events at different wavelengths in the infrared spectral range (indicated in the legend), extracted from the magnification maps presented in Fig. 11 (Stalevski et al. 2012).*

The corresponding timescales were in the range from several decades to several hundreds of years and, therefore, microlensing would hardly prove to be a practical tool to study and constrain the properties of dusty tori. However, these results should be kept in mind when investigating the flux anomaly of lensed quasars.

4.3. Cosmological distribution of gravitational microlenses

The probability of observing a gravitational lensing event is usually expressed in terms of the optical depth τ (see e.g. Popović et al. 2003b, Zakharov et al. 2004). The optical depth τ (the chance of seeing a gravitational lens) is the probability that at any instant of time a distant source is covered by the Einstein ring of a deflector. In order to consider the contribution of gravitational microlenses in the X-ray variability of high redshifted quasars, we investigated their optical depth assuming they are located in bulges or/and in halos of such quasars, as well as at cosmological distances between the observer and these quasars (Zakharov et al. 2004).

We showed that the optical depth for cosmologically distributed microlenses depends on three cosmological parameters Ω_0, Ω_Λ, and Ω_L, corresponding to the mass density of the Universe at the present epoch, cosmological constant Λ, and the matter fraction in compact lenses, respectively. For the first two parameters we assumed nowadays widely accepted values $\Omega_0 \approx 0.3$ and $\Omega_\Lambda \approx 0.7$ (see Jarosik et al. 2011), and then we studied the optical depth in the following three cases (Zakharov et al. 2004):

(i) a small fraction of baryonic matter (25 %) forms microlenses ($\Omega_L = 0.01$);

(ii) almost all baryonic matter forms microlenses ($\Omega_L = 0.05$);

(iii) about 30% of non-baryonic (dark) matter forms microlenses ($\Omega_L = 0.1$).

The obtained results are graphically presented in Fig. 13 as a function of redshift, and the corresponding numerical values are given in Table 2 (Zakharov et al. 2004).
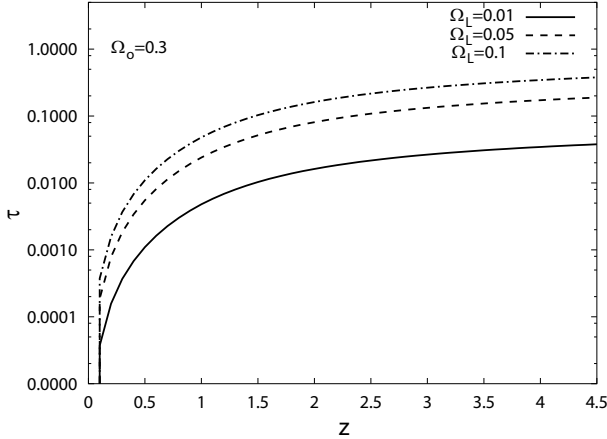

Fig. 13. *The optical depth for cosmologically distributed gravitational microlenses as a function of redshift for 3 different values of Ω_L and for $\Omega_0 = 0.3$ (Zakharov et al. 2004).*

Table 2. Numerical values of the microlensing optical depth presented in Fig. 13 (Zakharov et al. 2004).

$z\backslash\Omega_L$	0.01	0.05	0.10
0.5	0.001100	0.005499	0.010998
1.0	0.004793	0.023967	0.047934
1.5	0.010310	0.051550	0.103100
2.0	0.016196	0.080980	0.161959
2.5	0.021667	0.108334	0.216669
3.0	0.026518	0.132590	0.265180
3.5	0.030770	0.153852	0.307703
4.0	0.034504	0.172521	0.345042
4.5	0.037804	0.189018	0.378037
5.0	0.040742	0.203712	0.407424

These results show that the optical depth for cosmologically distributed microdeflectors could be significant and, hence, they could significantly contribute to the X-ray variability of high-redshifted ($z > 2$) quasars (Zakharov et al. 2004). Taking into account that the upper limit of the optical depth corresponds to the case where the dark matter forms cosmologically distributed deflectors, one can conclude that the gravitational microlensing can be used as a tool to estimate the dark matter fraction in the Universe.

5. DARK MATTER AND/OR MODIFIED GRAVITY

According to the standard ΛCDM cosmological model, the dark matter that we cannot detect by any other means except by gravitational lensing, constitutes about 5/6 of the total mass of the Universe, while the visible or baryonic matter contributes with only 1/6 (Jarosik et al. 2011). It is believed that the dark matter is, in large part, composed of non-baryonic particles with very small primordial velocity dispersion, which are so weakly interacting that they move purely under the influence of gravity (see e.g. Zacek 2008).

Flat rotation curves of spiral galaxies are usually assumed to be the most significant observational evidence for the dark mater hypothesis (Binney and Tremaine 2008). Namely, rotation curves of most spiral galaxies cannot be explained by their detected baryonic mass and the Newtonian gravitational force law and, therefore, the dark matter hypothesis tries to explain this problem by assuming the existence of a spherical dark matter halo. According to this hypothesis, during a merger of two galactic clusters, the weakly interacting dark matter should be mostly concentrated in outer regions and there should be the offset between the dark and visible matter distribution peaks. This was indeed inferred from a weak lensing mass reconstruction in the case of the famous "Bullet Cluster" - 1E 0657-558, which was considered as the first empirical evidence for the existence of dark matter (Clowe et al. 2006).

However, some recent studies of dark matter based on gravitational lensing discovered anomalies in its distribution, which are not completely in accordance with the previous assumptions, e.g. in the case of Abell 520, whose core is probably composed of dark matter (Mahdavi et al. 2007). Also, some very recent observational studies of gas rich galaxies contradict the dark matter hypothesis. Namely, an empirical relation between the observed mass (or luminosity) and nearly constant velocity at the flat part of rotational curve of a spiral galaxy, the so called Tully-Fisher relation (Binney and Tremaine 2008), is one of the most convincing probes for the dark matter content of such a galaxy. Recently, the baryonic Tully-Fisher relation has been tested for gas rich galaxies (McGaugh 2011). This is the most rigorous observational test that has been taken until now because the mass of gas rich galaxies can be measured much more precisely than the mass of most other galaxies where stars dominate the baryonic mass budget. The obtained results have large discrepancy with predictions of the ΛCDM cosmological model (see Fig. 2 in McGaugh 2011). At the same time, the observations behave precisely as predicted by the modified Newtonian dynamics (MOND) (Milgrom 1983), which excludes the existence of dark matter in these galaxies. Until now, this is one of the most significant observational challenges to the standard cosmological model in which the dark matter is one of the corner stones.

Basically, there are two possible approaches to explain these observed anomalies (Jovanović 2012b):

  (i) The standard approach which assumes the existence of dark matter, but with necessary revision of its nature and interaction with baryonic matter (see e.g. Cyburt et al. 2002).

  (ii) The alternative approach, which proposes different modifications of the fundamental gravitational and/or dynamical laws on the galactic scales, such as: MOND, scalar-tensor, conformal, Yukawa-like and R^n modified gravity, etc. (see e.g. Zakharov et al. 2006 and references therein), in order to exclude the need for dark matter.

As it can be seen from the previous section, within the frame of the standard approach, we investigated the dark matter and its distribution at different scales by using the gravitational lensing phenomenon. However, one part of our current investigations is also related to the alternative approach, since we also study some modified theories of gravity (Jovanović 2012b, Borka et al. 2012).

5.1. Modified gravity and S-stars

The extended theories of gravity have been proposed as alternative approaches to the Newtonian gravity on the basis of data from the Solar system, binary pulsars, spiral galaxies, clusters of galaxies and the large-scale structure of the Universe. One form of these extended theories of gravity are power-law fourth-order theories, one representative of which is the R^n gravity where the gravitational potential is given by (Capozziello et al. 2006, 2007):

$$\Phi(r) = -\frac{GM}{2r}\left[1 + \left(\frac{r}{r_c}\right)^{\beta}\right],$$

where r_c is an arbitrary parameter depending on the typical scale of the considered system, and β is a new universal constant. As expected, for $\beta = 0$ the R^n gravitational potential reduces to the Newtonian one. However, Capozziello et al. (2007) found a very good agreement between the theoretical rotation curves and the data using the value $\beta = 0.817$, which was obtained by fitting the SN Ia Hubble diagram with a model comprising only the baryonic matter but regulated by the modified Friedmann equations derived from the R^n gravity Lagrangian.

We studied possible application of the R^n gravity at Galactic scales to explain the recently observed precession of orbits of S-stars, as well as whether these observations could be used for constraining this type of modified gravity. S-stars are the bright stars, which move around the center of our Galaxy where the compact radio source Sgr A* is located, and they provide the most convincing evidence that Sgr A* represents a massive black hole (see

Meyer et al. 2012 and references therein). For one of these stars, labeled S2, there are some observational indications that its orbit deviates from the Keplerian one due to orbital precession. This orbital precession can be relativistic and, hence, prograde, or Newtonian due to potential extended mass distribution and, hence, retrograde. Both, the prograde and retrograde pericentre shifts result in rosette shaped orbits.

To test whether the R^n gravity is able to provide a reasonable explanation for this orbital precession of S2 star, we simulated its orbit in the R^n gravitational potential. A comparison between the simulated orbits in the Newtonian and R^n gravity is presented in Fig. 14 (Jovanović 2012b). From this figure one can see that the R^n gravity also causes a retrograde pericenter shift, which results in rosette shaped orbits of S2 star (Borka et al. 2012).
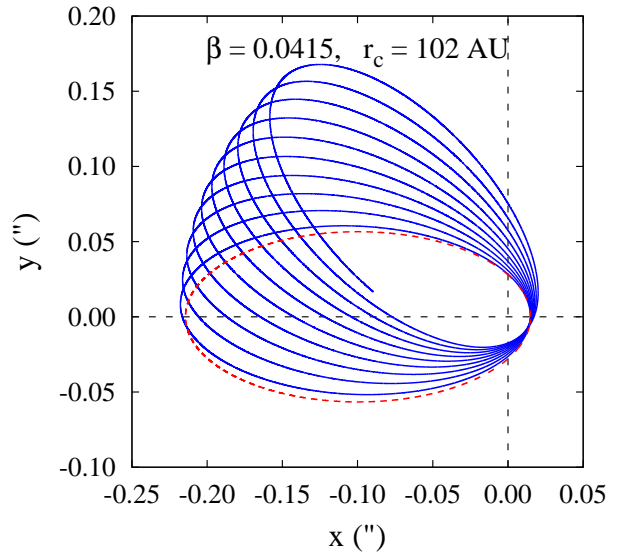

Fig. 14. *The simulated orbits of S2 star in the Newtonian (red dashed line) and R^n gravity (blue solid line) for $r_c = 102$ AU and $\beta = 0.0415$ during 10 orbital periods (Jovanović 2012b).*

We then compared these theoretical results with two independent sets of observations of S2 star, obtained by the New Technology Telescope/Very Large Telescope (NTT/VLT), as well as by the Keck telescope (Gillessen et al. 2009). The best fit was obtained for a small value of the universal constant $\beta = 0.01$ (and hence for precession per orbital period of around $-1°$), and the corresponding comparisons between the simulated positions and those observed by the NTT/VLT and Keck are presented in left and middle panels of Fig. 15, respectively (Borka et al. 2012). A comparison between the fitted and observed radial velocities of S2 star is given in the right panel of the same figure.
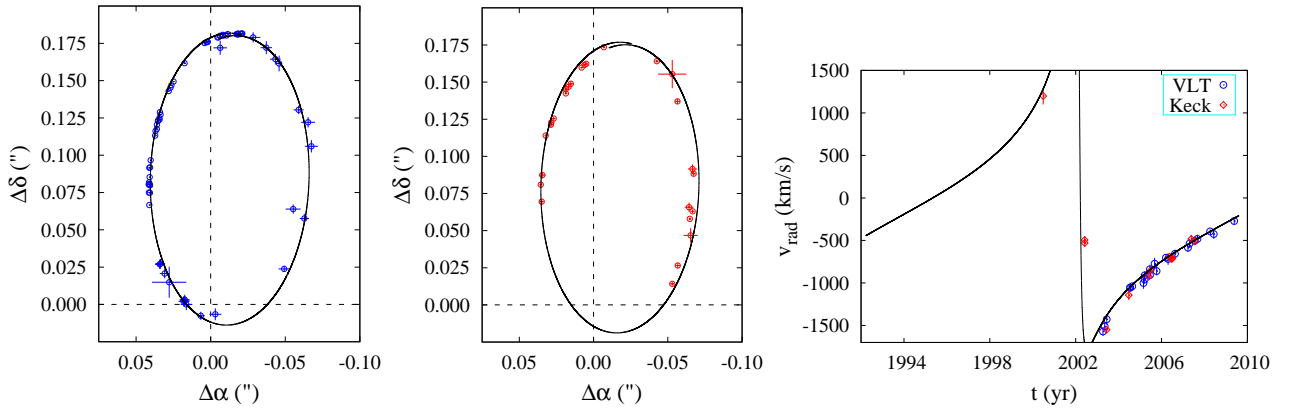
Fig. 15. *The fitted orbit of S2 star around a massive black hole at Galactic center in the R^n gravity for $r_c = 100$ AU and $\beta = 0.01$ (black solid lines in first two panels). The NTT/VLT astrometric observations are presented in the left panel by blue circles, while the Keck measurements are denoted by red circles in the middle panel (Borka et al. 2012). Right panel presents a comparison between the fitted (black solid line) and observed radial velocities of S2 star. Observed values are denoted by circles (VLT) and diamonds (Keck).*

According to these results one can conclude that despite of an excellent agreement between theoretical and observed rotation curves obtained by Capozziello et al. (2007), and despite of its ability to fit satisfactorily the orbit of S2 star around the central SMBH of our Galaxy (Borka et al. 2012), the R^n gravity may not represent a good candidate to solve both the dark energy problem on cosmological scales and the dark matter one on galactic scales since different values for the universal constant β are needed for these two scales.

6. CONCLUSIONS

In this paper we presented a short overview of our investigations of the following galactic and extragalactic gravitational phenomena: supermassive black holes in the centers of galaxies and quasars, supermassive black hole binaries, gravitational lenses, dark matter and modified gravity as its potential alternative. The most important results of these studies can be summarized as follows:

(i) We developed a model of a relativistic accretion disk around a SMBH, based on the ray-tracing method in Kerr metric. Using this model we simulated radiation in different spectral bands from such accretion disks located in centers of active galaxies and quasars. Comparisons of these simulations with observations enabled us to study physics, spacetime geometry, and effects of strong gravity in the the vicinity of SMBHs.

(ii) To investigate the observed variability in radiation from active galaxies and quasars, we developed a model of emissivity perturbations in the form of a bright spot or flare in the accretion disk. It was shown that this model can successfully explain the variability of some active galaxies. Furthermore, we used this bright spot model to study photocentric variability and astrometric stability of quasars in the context of the future Gaia mission. The obtained results showed that bright spots in accretion disks could cause offsets of quasar photocenters by a few mas which will be detectable by Gaia.

(iii) We studied observational signatures of SMBHBs and found evidence for the first spectroscopically resolved sub-parsec orbit of a such system in the core of active galaxy NGC 4151. The obtained results also suggested that many such SMBHBs may exist in similar active galaxies, whose binarity could be a necessary condition for triggering their activity.

(iv) Gravitational lenses were an important subject of our investigations, which included both the observational, as well as theoretical studies of their different aspects. Our theoretical investigations were mostly focused on gravitational microlenses and their influence on radiation from relativistic accretion disks around the central SMBHs of distant quasars, their cosmological distribution and statistics, as well as their influence on radiation in different spectral bands emitted from lensed quasars with multiple images. To investigate these effects, we developed three different microlensing models: the point-like microlens, straight-fold caustic, and microlensing maps. We found that gravitational microlensing can produce significant variations and amplifications of radiation in the X-ray, UV, optical and infrared spectral bands. Even very compact microlenses could produce noticeable changes in the X-ray radiation, which originate in the vicinity of SMBHs and this makes gravitational microlensing a powerful tool for investigation of the innermost parts of relativistic accretion disks and for scanning the inner regions of active galaxies and quasars. Although the gravitational microlensing is an achromatic effect, it can induce wavelength de-

13

pendent variations in the X-ray, UV, optical and infrared spectral bands due to different sizes of their emitting regions. However, the variations in the X-ray band are the strongest and fastest in comparison with other bands. We also showed that the optical depth for cosmologically distributed microlenses could be significant in the case where the dark matter forms compact objects and, thus, gravitational microlensing can be used as a tool for estimating the dark matter fraction in the Universe.

(v) We also studied an alternative to the dark matter in the form of the R^n theory of modified gravity, and its possible applications at Galactic scales to explain the observed orbital precession of some, so called, S-stars which are orbiting around a massive black hole at Galactic center. The obtained results show that, in spite of its ability to satisfactorily explain this precession of S-stars, the R^n gravity may not represent a good candidate to solve both the dark energy problem on cosmological scales and the dark matter one on galactic scales, since different values for the new universal constant β are needed for these two scales.

REFERENCES

Baes, M., Davies, J. I., Dejonghe, H., et al.: 2003, *Mon. Not. R. Astron. Soc.*, **343**, 1081.

Binney, J. and Tremaine, S.: 2008, Galactic Dynamics: Second Edition, Princeton University Press, Princeton, NJ USA

Bogdanović, T., Smith, B. D., Sigurdsson, S., and Eracleous, M.: 2008, *Astrophys. J. Suppl. Series*, **174**, 455.

Bogdanović, T., Eracleous, M., and Sigurdsson, S.: 2009, *New Astron. Rev.*, **53**, 113.

Bon, E., Popović, L. Č., Gavrilović, N., La Mura, G. and Mediavilla, E.: 2009, *Mon. Not. R. Astron. Soc.*, **400**, 924.

Bon, E., Jovanović, P., Marziani, P., Shapovalova, A. I., Bon, N., Borka Jovanović, V., Borka, D., Sulentic, J., Popović, L. Č: 2012, *Astrophys. J.*, **759**, 118.

Borka, D., Jovanović, P., Borka Jovanović, V., Zakharov, A. F.: 2012, *Phys. Rev. D*, **85**, 124004.

Bourda, G., Charlot, P., Porcas, R. W., and Garrington, S. T.: 2010, *Astron. Astrophys.*, **520**, A113.

Cao, S., Covone, G., Zhu, Z.-H.: 2012, *Astrophys. J.*, **755**, 31.

Capozziello, S., Cardone, V. F., Troisi A.: 2006, *Phys. Rev. D*, **73**, 104019.

Capozziello, S., Cardone, V. F., Troisi A.: 2007, *Mon. Not. R. Astron. Soc.*, **375**, 1423.

Clowe, D., Bradač, M., Gonzalez, A. H., et al.: 2006, *Astrophys. J.*, **648**, L109.

Cyburt, R. H., Fields, B. D., Pavlidou, V., and Wandelt, B.: 2002, *Phys. Rev. D*, **65**, 123503.

Gambill, J. K., Sambruna, R. M., Chartas, G., et al.: 2003, *Astron. Astrophys.*, **401**, 505.

Gillessen, S., Eisenhauer, F., Fritz, T. K., et al.: 2009, *Astrophys. J.*, **707**, L114.

Goldberg, D. M., Chessey, M. K., Harris, W. B., Richards, G. T.: 2010, *Astrophys. J.*, **715**, 793.

Ingrosso, G., Novati, S. C., de Paolis, F., et al.: 2009, *Mon. Not. R. Astron. Soc.*, **399**, 219.

Jackson, N.: 2007, *Living Reviews in Relativity*, **10**, 4.

Jarosik, N., Bennett, C. L., Dunkley, J., et al.: 2011, *Astrophys. J. Suppl. Series*, **192**, 14.

Jovanović, P.: 2005, *Mem. S.A.It. Suppl.*, **7**, 56.

Jovanović, P.: 2006, *Publ. Astron. Soc. Pac.*, **118**, 656.

Jovanović, P.: 2012a, *New Astron. Rev.*, **56**, 37.

Jovanović, P.: 2012b, *Rom. Journ. Phys.*, **57**, Nos. 5–6, 873.

Jovanović, P. and Popović, L. Č.: 2008a, *Fortschritte der Physik*, **56**, 456.

Jovanović, P. and Popović, L. Č.: 2008b, *Publ. Astron. Obs. Belgrade*, **84**, 467.

Jovanović, P. and Popović, L. Č.: 2009a, in "Black Holes and Galaxy Formation", eds. Adonis D. Wachter and Raphael J. Propst, Nova Science Publishers Inc, Hauppauge NY, USA, 249.

Jovanović, P. and Popović, L. Č.: 2009b, *Publ. Astron. Soc. "Rudjer Bošković"*, **9**, 45.

Jovanović, P. and Popović, L. Č.: 2010, *Publ. Astron. Obs. Belgrade*, **88**, 91.

Jovanović, P., Popović, L. Č., Dimitrijević, M. S.: 2003, *Publ. Astron. Obs. Belgrade*, **76**, 205.

Jovanović, P., Zakharov, A. F., Popović, L. Č. and Petrović, T. 2008, *Mon. Not. R. Astron. Soc.*, **386**, 397.

Jovanović, P., Popović, L. Č., Simić, S.: 2009, *New Astron. Rev.*, **53**, 156.

Jovanović, P., Popović, L. Č., Stalevski, M. and Shapovalova, A. I.: 2010, *Astrophys. J.*, **718**, 168.

Jovanović, P., Borka Jovanović, V., and Borka, D.: 2011, *Balt. Astron.*, **20**, 468.

Lindegren, L., Babusiaux, C., Bailer-Jones, C., Bastian, U. et al.: 2008, *IAU Symposia*, **248**, 217.

Mahdavi, A., Hoekstra, H., Babul, A., Balam, D. D. and Capak, P. L.: 2007, *Astrophys. J.*, **668**, 806.

Massey, R., Rhodes, J., Ellis, R., et al.: 2007, *Nature*, **445**, 286.

McGaugh, S. S.: 2011, *Phys. Rev. Lett.*, **106**, 121303.

Meyer, L., Ghez, A. M., Schödel, R., et al.: 2012, *Science*, **338**, 84.

Milgrom, M.: 1983, *Astrophys. J.*, **270**, 365.

Mortonson, M. J., Schechter, P. L., and Wambsganss, J.: 2005, *Astrophys. J.*, **628**, 594.

Oguri, M., Inada, N., Strauss, M. A., et al.: 2012, *Astron. J.*, **143**, 120.

Onken, C. A., Valluri, M., Peterson, B., M., Pogge, R., W., Bentz, M., C., Ferrarese, L., Vestergaard, M., Crenshaw, D. M,. Sergeev, S., G., McHardy, I., M. et al.: 2007, *Astrophys. J.*, **670**, 105.

Perryman, M. A. C., de Boer, K. S., Gilmore, G., et al.: 2001, *Astron. Astrophys.*, **369**, 339.

Popović, L. Č.: 2012, *New Astron. Rev.*, **56**, 74.

Popović, L., Č., Mediavilla, E. G., Muñoz J., Dimitrijević, M. S., Jovanović, P.: 2001, *Serb. Astron. J*, **164**, 73.

Popović, L. Č, Jovanović, P., Mediavilla, E., Muñoz, J. A.: 2003a, *Astron. Astrophys. Trans.*, **22**, 719.

Popović, L. Č., Mediavilla, E. G., Jovanović, P., Muñoz, J. A.: 2003b, *Astron. Astrophys.*, **398**, 975.

Popović, L. Č., Jovanović, P., Mediavilla, E., et al. 2006, *Astrophys. J.*, **637**, 620.

Popović, L. Č., Moiseev, A. V., Mediavilla, E., Jovanović, P., Ilić, D., Kovačević, J., Muñoz, J. A.: 2010, *Astrophys. J.*, **721**, L139.

Popović, L. Č., Jovanović, P., Stalevski, M., et al.: 2012, *Astron. Astrophys.*, **538**, A107.

Richard, J., Kneib, J.-P., Ebeling, H., et al.: 2011, *Mon. Not. R. Astron. Soc.*, **414**, L31.

Simić, S., Popović, L. Č., Jovanović, P.: 2011, *Balt. Astron.*, **20**, 481.

Stalevski, M., Jovanović, P., Popović, L. Č.: 2008, *Publ. Astron. Obs. Belgrade*, **84**, 491.

Stalevski, M., Jovanović, P., Popović, L. Č., Baes, M.: 2012, *Mon. Not. R. Astron. Soc.*, **425**, 1576.

Stark, D. P., Ellis, R. S., Richard, J., et al.: 2007, *Astrophys. J.*, **663**, 10.

Wald, R. M.: 1984, General relativity, University of Chicago Press, Chicago

Wilson, A. S., Young, A. J., Shopbell, P. L.: 2001, *ASP Conf. Proc.*, **250**, 213.

Yaqoob, T.: 2007, *ASP Conf. Ser.*, **373**, 109.

Zacek, V.: 2008, Fundamental Interactions: Proceedings of the 22nd Lake Louise Winter Institute, 170.

Zakharov, A. F.: 2009, *New Astron. Rev.*, **53**, 202.

Zakharov, F., Popović, L. Č., Jovanović, P.: 2004, *Astron. Astrophys.*, **420**, 881.

Zakharov, A. F., Popović, L. Č., Jovanović, P.: 2005, *IAU Symposia*, **225**, 363.

Zakharov, A. F., Nucita, A. A., de Paolis, F., and Ingrosso, G.: 2006, *Phys. Rev. D*, **74**, 107101.

ИСТРАЖИВАЊЕ НЕКИХ ГАЛАКТИЧКИХ И ВАНГАЛАКТИЧКИХ ГРАВИТАЦИОНИХ ПОЈАВА

P. Jovanović

Astronomical Observatory, Volgina 7, 11060 Belgrade 38, Serbia
E–mail: *pjovanovic@aob.rs*

У овом раду је представљен преглед најважнијих резултата наших истраживања следећих галактичких и вангалактичких гравитационих појава: супермасивних црних рупа у центрима галаксија и квазара, двојних супермасивних црних рупа, гравитационих сочива и тамне материје. У циљу тих истраживања, развили смо модел релативистичког акреционог диска око супермасивне црне рупе који је заснован на методу праћења зрака у Кер метрици, модел сјајне пеге у акреционом диску, као и три различита модела гравитационих микросочива. Сви ови модели су нам омогућили да изучавамо физичке процесе, геометрију простор-времена и ефекте јаког гравитационог поља у близини супермасивних црних рупа, променљивост неких активних галаксија и квазара, разне појаве у квазарима са вишеструким ликовима насталим услед утицаја гравитационих сочива, као и удео тамне материје у космосу. Такође смо у језгру активне галаксије NGC 4151 нашли посматрачку потврду прве орбите двојног система супермасивних црних рупа на скалама испод једног парсека, која је раздвојена спектроскопски. Поред тога, испитивали смо и примену могуће алтернативе тамној материји у облику једне од модификованих теорија гравитације за објашњење недавно посматране орбиталне прецесије неких S-звезда које круже око масивне црне рупе у центру наше галаксије.